Sum-rate Performance of Large Centralized and Distributed MU-MIMO Systems in Indoor WLAN

Qing Wang, *Student Member, IEEE*, Diptanil Debbarma, Anthony Lo, Ignas Niemegeers, Sonia Heemstra de Groot

Abstract - Large MIMO systems are recognized as an effective technique for increasing the spectral and energy efficiency of wireless networks. The attractiveness of this technique for WLAN is that it can be an alternative approach to cell densification for providing high data rate wireless access. Here we consider large MIMO systems in indoor WLANs for multi-user MIMO (MU-MIMO) spatial multiplexing in the 2.4 GHz ISM band. The focus is on analyzing the behaviors of large MIMO systems with both centralized and distributed antenna system (CAS and DAS) architectures. The analysis is based on extensive ray-tracing channel simulations, as well as an i.i.d. Rayleigh model. The numerical results show that the optimum capacity can be closely approached with both CAS and DAS architectures when the number of Access Point (AP) antennas exceeds the users by a few times. DAS is found to be superior to CAS in that the required number of antennas is significantly smaller, and especially performs better in non-rich scattering channels which is the case of practical channels reflected by ray-tracing simulations.

Index Terms **– MU-MIMO, large MIMO, centralized antenna system, distributed antenna system, WLAN**

I. INTRODUCTION

Large MIMO has been advocated recently as a promising technique for next generation wireless networks due to its manifold benefits, especially the potential of a tremendous boost of spectral efficiency and energy efficiency [1] [2]. This technique brings at least two fundamental changes to the traditional MIMO scheme [1]. First, a large number of antennas are employed at the base station (BS) or access point (AP), say tens to hundreds or even more. Traditional MIMO systems typically have only a small number, e.g., maximally 8 in the latest WiFi standard IEEE 802.11ac (for frequency bands below 6 GHz). Potentially, the capacity can be increased multiple times with higher order spatial multiplexing in large MIMO. Second, the number of BS or AP antennas is much larger than the number of co-scheduled mobile stations (STAs), say 10 times more. Traditional MIMO systems usually assume a similar or equal numbers of transmit and receive antennas. The additional antennas make it possible to use linear precoding to achieve high data rate, which reduces the signal processing complexity in high-dimensional MIMO. Large MIMO has now been recognized as a promising technique for next-generation cellular networks or 5G, however, its use in WLAN is rarely discussed in the literature at this time.

The attractiveness of large MIMO for WLAN is that it can be an alternative approach for cell densification to provide high data rate access, especially for high user density scenarios like airport gates, train stations, crowded office buildings, etc. A basic problem of cell densification is that the network may have degraded performance by intra- and inter-cell interference due to poorly-coordinated transmissions. On the contrary, in large MIMO, the cooperation of a large number of antennas can sharply focus signals onto the intended users and cancel the undesired signals in almost all other directions. As a result, not only a larger number of parallel spatial streams can be supported but also the data rate of each stream can be significantly improved to guarantee the quality-of-service (QoS) for simultaneously served users.

The objective of this paper is to analyze the behavior of large MIMO systems in WLAN, and verify the viability of achieving the optimum capacity with a reasonable number of antennas for multi-user MIMO (MU-MIMO) spatial multiplexing. Unlike cellular networks which consider outdoor environments, licensed frequency bands, and relatively large cells, WLAN mainly aims at indoor environments and applications, and use license-free bands. Therefore, the discussions in this paper differ from the prior work for cellular networks reported in [3] [4] [5]. Moreover, [3] and [4] only consider centralized antenna system (CAS) architecture, and [5] only uses theoretical channel models. Our work differs in another two aspects. First, we consider both CAS and DAS architectures. Second, we use both practical and theoretical MIMO channels, to highlight the performance differences in practical and ideal channel conditions. The practical indoor wireless channels are simulated by ray-tracing software, which can characterize large MIMO channels with good accuracy as verified in [6]. The theoretical MIMO channel model combines the i.i.d. Rayleigh small-scale fading model, and the path loss results obtained from ray-tracing simulations, to obtain the ideal channel condition. Above that, the deployment of the antennas is optimized based on the received signal strength over the coverage area to better fit antennas into the indoor environment. We find that, a large number of STAs can be supported simultaneously and achieve the optimum capacity with a limited number of antennas for both CAS and DAS architectures. The results, however, show a significant advantage of DAS architecture over CAS, especially in practical channels.

The remainder of this paper is organized as follows. Section

Manuscript received: August 13, 2015. Revised: September 23, 2015.

Q. Wang, D. Debbarma, I. Niemegeers and S. Heemstra de Groot are with the Department of Electrical Engineering, Eindhoven University of Technology, Netherlands, (e-mail: {qing.wang, z.cao, d.debbarma, i.g.m.m.niemegeers, s.heemstradegroot}@tue.nl). A. Lo is with Universiti Teknologi Malaysia, Malaysia.

The work in this paper was partially supported by Dutch IOP Gencom MEANS project.

II provides the system model and the sum-rate capacity metrics for the subsequent analysis. Section III presents the channel simulation methods with a ray-tracing tool, and the modeling of the ideal MIMO channel. Section IV examines the numerical results we obtained. Section V concludes the paper and highlights remaining important issues that need to be investigated.

II. SYSTEM MODEL

We consider a single cell or single AP WLAN with CAS and DAS architectures, illustrated in Fig. 1. For DAS systems, the remote antenna units (RAUs) or antenna clusters are typically connected by wirelines to the AP. In particular, optical fiber is a promising wireline connection that has been advocated in recent years [7]. We denote the number of RAUs, the number of antennas per RAU, and the number of co-scheduled single-antenna STAs by M , N and K , respectively. So the total number of AP antennas is MN . CAS is taken as a special case that $M=1$, then N equals the total number of antennas.

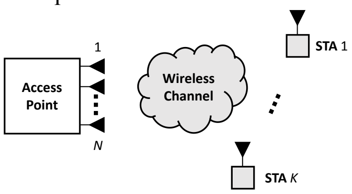

(a) Centralized antenna system

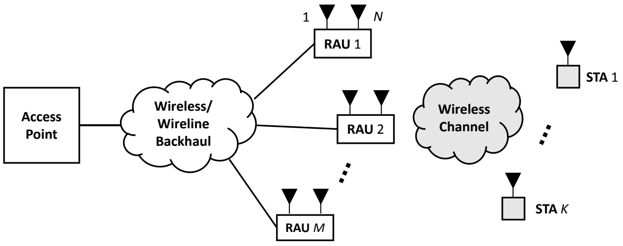

(b) Distributed antenna system

Fig. 1 Architecture of CAS and DAS for WLAN.

In a CAS, the antennas of an AP are co-located, typically with half-wavelength spacing between individual antennas. As a result, the antennas of the AP usually share the same large scale fading for the same user, and small scale fading variations are correlated across the antennas. The channel correlation renders the MIMO channel of low rank which limits the spatial multiplexing gain. So in traditional MIMO systems, user scheduling is used to select the users that are well separated spatially, so as to obtain more “favorable" MIMO channels. This requirement is however much relaxed in large MIMO [1].

In a DAS, the antennas are clustered in the RAUs, and the RAUs are scattered over the coverage area. The antenna separation in a RAU is small, typically with half-wavelength, but the RAUs are separated by distances of at least several meters. The MIMO system can then benefit from two facts. First, the macro-diversity due to the large separation of RAUs which reduces the average path loss to the users thus improves the average received signal strength. Second, the micro-diversity improves the independence of small scale fading across the antennas at different RAUs, which lowers MIMO channel correlation. Therefore, the DAS architecture is superior to the CAS architecture for traditional MIMO systems, which has been confirmed in the studies like [8]. Evidently, the cost is the higher complexity of the infrastructure.

The following assumptions are made for our modeling and analysis:

- The K co-scheduled STAs are selected by random scheduling, i.e., without optimization based on the spatial separability of the STAs, since large MIMO potentially can achieve the optimum performance without sophisticated user scheduling as in traditional MIMO systems. In addition, the STAs are uniformly distributed over the entire area. We leave the discussions on non-uniform distributions for our future research.
- We assume global sum power constraint over all the antennas. This assumption leads to a much lower complexity in computing the precoding matrix [9]. In addition to that, we also argue that the transmission power of the antennas is extremely low in large MIMO systems due to the high beamforming gain with the numerous antennas and the reduced path loss in DAS systems especially for indoor WLAN setups, which makes the assumption also reasonable in practice.
- To simplify the analysis, we assume the backhaul connection in the DAS architecture is ideal. For example, delays across the RAUs are assumed equal and the bandwidth is sufficiently large; optical fiber distortions are already compensated [10]. In addition, the constraints like channel estimation accuracy and power regulations on EIRP, are not considered in order to keep a clear focus in the analysis.

A. Signal Model

The signal model is given in the following for block-fading narrow-band channels. The block-fading channel model is suitable for indoor channels due to the slow user mobility and physical environment changes. The extension of the narrow band model to OFDM systems is straightforward. In the numerical analysis, we will consider OFDM modulation, and use equal power allocation to the subcarriers. In addition, the models are given assuming perfect channel knowledge is known.

Denote the full channel matrix by $\mathbf{G}=[\mathbf{g}_1,\cdots,\mathbf{g}_K]$, where $\mathbf{g}_k, k=1,\cdots,K$ is the channel vector of the k th STA. The channel coefficients consist of both large scale fading and small scale fading. Specifically,

$$\mathbf{g_k}=\left[\beta_{1k}\mathbf{h}_{1k}^T,\cdots,\beta_{Mk}\mathbf{h}_{Mk}^T\right]^T \quad (1)$$

where β_{mk} is the large scale fading and $\mathbf{h}_{mk}$ is the small scale fading vector between the m th RAU and the k th STA, respectively. The received signal at the STAs is

$$\mathbf{y}=\mathbf{G}^H\mathbf{x}+\mathbf{n} \quad (2)$$

where $\mathbf{x}$ is the precoded signal vector, $\mathbf{n}$ is the Gaussian noise vector with i.i.d. elements following $\mathcal{CN}(0,\sigma^2)$ and σ^2 is the noise power.

B. Sum-rate Capacity

Sum-rate capacity is the total achievable data rate of all the co-scheduled STAs (measured in bps/Hz). In this paper, it is evaluated under different conditions to give a comprehensive view. Specifically, we take into account of the interference-free (IF) case, and different precoding techniques including DPC (Dirty Paper Coding), ZF (Zero-forcing) and MBF (matched beamforming), which are elaborated in the following.

1) IF

IF capacity is the best performance that can be achieved if all the channel energy to STA k is delivered to STA k but without any multi-user interference (MUI), which is usually used as a benchmark [1]. With such assumption, the data rate for the k th STA is given by

$$R_{\mathrm{IF},k} = \log_2\left(1+\frac{p_k \|\mathbf{g}_k\|^2}{\sigma^2}\right) \tag{3}$$

where p_k is the transmission power allocated for the k th STA, which is assumed to be equal for all STAs, so $p_k = P_t / K$, for $k = 1,\cdots,K$ and P_t is the total transmission power. The sum-rate is then given by

$$C_{\mathrm{sum,IF}} = \sum_{k=1}^{K} R_{\mathrm{IF},k} \tag{4}$$

2) DPC

DPC is the optimum non-linear precoding technique which gives the upper bound capacity for a given channel. The sum-rate is usually given in the following form

$$C_{\mathrm{sum,DPC}} = \max_{\mathbf{P}} \log_2 \det\left(\mathbf{I}+\frac{1}{\sigma^2}\mathbf{G}\mathbf{P}\mathbf{G}^H\right) \tag{5}$$

where $\mathbf{P}$ is a diagonal matrix representing the power allocation to the STAs, i.e., $\mathbf{P} = \mathrm{diag}\{p_1,\cdots,p_K\}$, constrained by $\sum_{k=1}^{K} p_k = P_t$. The optimum power allocation can be found by the water-filling algorithm [4]. In the high SNR regime, it can be approximated by [11]

$$C_{\mathrm{sum,DPC}} = \log_2 \det\left(\mathbf{I}+\frac{P_{\mathrm{total}}}{K\sigma^2}\mathbf{G}\mathbf{G}^H\right) \tag{6}$$

i.e., with equal power allocations to the STAs.

3) Linear Precoding

Linear precoding techniques are more favorable in practice due to their low complexity. In this paper, we consider ZF and MBF, which precode the signal with different objectives. Specifically, ZF only cancels MUI but neglecting the final SINRs of the STAs, and MBF only considers SNR maximization for individual STAs but without taking into account MUI. Although suboptimal, they are potentially able to achieve the optimum capacity performance in large MIMO regime, i.e., when $MN \gg K$ (see [1] for more information).

For linear precoding, we can write the received signal model as

$$\mathbf{y} = \mathbf{G}^H \mathbf{W} \mathbf{P}^{1/2} \mathbf{s} + \mathbf{n} \tag{7}$$

where $\mathbf{s}$ is the information symbol, and $\mathbf{W}$ is the beamforming matrix. Therefore, the SINR of the k th STA is given by

$$\mathrm{SINR}_k = \frac{|\mathbf{g}_k^H \mathbf{w}_k|^2 \, p_k}{\sum_{j\neq k} |\mathbf{h}_k^H \mathbf{w}_j|^2 \, p_j + \sigma^2} \tag{8}$$

The beamforming matrix $\mathbf{W}$ is obtained through the following procedure. First, the precoding matrices of MBF and ZF are calculated by

$$\tilde{\mathbf{W}}_{\mathrm{MBF}} = \mathbf{G} \tag{9}$$

$$\tilde{\mathbf{W}}_{\mathrm{ZF}} = \mathbf{G}(\mathbf{G}^H\mathbf{G})^{-1} \tag{10}$$

Then, the columns are normalized to achieve unit power of beamforming vectors. Specifically, in the final beamforming matrices, $\mathbf{W}_{\mathrm{ZF}}$ and $\mathbf{W}_{\mathrm{MBF}}$, the columns are obtained by $\mathbf{w}_k = \tilde{\mathbf{w}}_k / \|\tilde{\mathbf{w}}_k\|$. Since for ZF, $\mathbf{h}_i^H \mathbf{w}_j = 0$ for $i \neq j$, the first term of the denominator of the Eq. (8) will be zero.

Finally, the sum-rate is calculated by

$$C_{\mathrm{sum,ZF/MBF}} = \sum_{k=1}^{K} \log_2(1+\mathrm{SINR}_{k,\mathrm{ZF/MBF}}) \tag{11}$$

In addition, equal power allocation is assumed for the linear precoders as well in the analysis.

III. CHANNEL MODELS

Channel modeling is important for investigating the performance of MIMO systems. As already pointed out in [4] [12], the channel conditions of the STAs, e.g., line-of-sight (LOS) and none-line-of-sight (NLOS), have noticeable effect on the achievable data rates. In this paper, both ray-tracing channel simulation and an ideal channel model are used. Ray-tracing simulation based channel modeling stands for the characterization of more practical channels, in contrast to the ideal channel condition.

A. Ray-tracing Simulation

The ray-tracing simulations are conducted in a 3D ray-tracing tool named Radiowave Propagation Simulator (RPS) [13]. To make the simulations more scalable, the channel transfer functions are derived with the following steps. First, the locations of the M RAUs are optimized according to received signal strength. Specifically, we locate the RAUs on 5m grids on the ceiling plane of the indoor scenario (see Fig. 2), assuming each RAU has a single isotropic antenna and the same transmission power. Then, the group of RAU positions that provides the highest 5-percentile receive signal power over the entire coverage area is selected. The searching algorithm used here is “greedy search”, which iteratively adds one RAU to maximize the objective function (see [14] for more details). A reason why we choose this algorithm is that it is deterministic, which yields reproducible optimization results. Second, the band-limited time-domain channel impulse responses (CIR) between each RAU and each STA position are derived from RPS, along with angular (departure and arrival angles) and temporary information of all the rays. Third, the channels of each sub-antenna array, i.e., the antennas on each RAU (organized as a uniform planar array), are obtained by adding the array response to the CIRs derived from the last step. See [6] for more explanations which also verifies the effectiveness of this approach. Finally, the

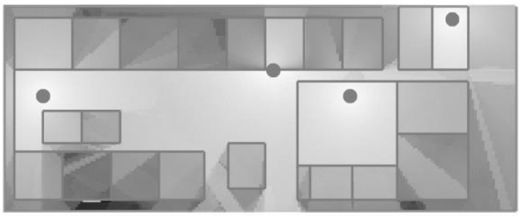

Fig. 2 Simulation scenario with an example of four RAUs deployed at optimized positions, the dots in the figure. The color map shows the received signal strength when assuming 0 dBm transmission power at each RAU.

channel transfer functions on the subcarrier are derived by applying Fast Fourier Transform (FFT) on the CIRs of all antennas.

The selected scenario is a floor of the Electrical Engineering (Flux) building of Eindhoven University of Technology where most of the rooms are for lectures and laboratories, of dimension 100 m × 40 m × 4 m, which is illustrated in Fig. 2. The main objects considered in the ray-tracing simulations are the walls, floor and ceiling. The walls are plastered, and ceilings and floors are concrete, typical materials of large surfaces of office buildings.

B. Ideal Channel Model

The wireless channel model is, as usual, divided into large scale fading and small scale fading. Here the small scale fading across the antennas at an RAU for an STA is described by the i.i.d. Rayleigh fading model. I.i.d. Rayleigh fading model represents the physical environments that are rich in scatters, which somehow results in the ideal channel condition for multi-user spatial multiplexing [3], which results in a capacity upper bound. To be consistent with ray-tracing channel simulation, we have to force the receive signal power between any pair of STA and RAU at the subcarriers to be the same. Therefore, we derive the the ideal channel through the following procedure.

First, we denote the average channel gain between the m th RAU and the k th STA from ray-tracing channel simulation by β_{mk}, which is obtained by the following normalization

$$\beta_{mk}^{\mathrm{RT}} = \frac{\sum_{l=1}^{L} \| \mathbf{g}_{mk}^{\mathrm{RT}}[l] \|_{\mathrm{F}}^2}{NL} \tag{12}$$

where $\|\cdot\|_{\mathrm{F}}$ is Frobenius norm. $\mathbf{g}_{mk}^{\mathrm{RT}}[l]$ is the channel vector on the l th subcarrier, and $l = 1, \cdots, L$ (RT is short for ray-tracing). As a result, the small scale fading $\mathbf{h}_{mk}^{\mathrm{RT}}[l] = \mathbf{g}_{mk}^{\mathrm{RT}}[l] / \beta_{mk}^{\mathrm{RT}}$ will have unit average power over all the N antennas and L subcarriers. Note that this channel gain is obtained from an instantaneous channel, which is different from the common large scale fading factor derived by long-term average.

Then, we denote the small scale fading of i.i.d. Rayleigh channel as $\mathbf{h}_{mk}^{\mathrm{IID}}[l]$, where the elements follow i.i.d. $\mathcal{CN}(0,1)$. It is then normalized by

$$\bar{\mathbf{h}}_{mk}^{\mathrm{IID}}[l] = \sqrt{\frac{NL}{\sum_{l=1}^{L} \| h_{mk}^{\mathrm{IID}}[l] \|_{\mathrm{F}}^2}} \mathbf{h}_{mk}^{\mathrm{IID}}[l] \tag{13}$$

to obtain unit average power over all the antennas and subcarriers.

Finally, the i.i.d. Rayleigh MIMO channel used for analysis is derived by

$$\mathbf{g}_{mk}^{\mathrm{IID}}[l] = \beta_{mk}^{\mathrm{RT}} \bar{\mathbf{h}}_{mk}^{\mathrm{IID}}[l] \tag{14}$$

As a result, the ray-tracing channel $\mathbf{g}_{mk}^{\mathrm{RT}}[l]$ and i.i.d. Rayleigh channel $\mathbf{g}_{mk}^{\mathrm{IID}}[l]$ will give the same receive power over all subcarriers provided the same total transmission power. The reader can refer to [4] for more details about channel normalization techniques.

IV. NUMERICAL RESULTS

This section presents the numerical results based on the above models to analyze the influences of different parameters on the sum-rate. We consider the antenna system architectures, the precoding techniques and the physical channels. We try to seek insights for the following questions: (1) how many antennas are needed to support a certain number of STAs (2) how differently does large MIMO behave under practical and ideal channel conditions (3) what is the performance difference between CAS and DAS architectures (4) how do the precoding techniques perform. These questions are interesting for practical implementations.

The common simulation parameters are given in Table I.

TABLE I SIMULATION PARAMETERS

Frequency	2.4 GHz
Bandwidth	20 MHz
Number of subcarriers	64
Background noise	-174 dBm/Hz
Noise figure	10 dB
Transmission power	P_0=20 dBm (equal allocation to subcarriers)
Scenario	100 m×40 m× 4 m (STAs at 1 m height)

A. Capacity Versus Number of AP Antennas

We first analyze the influence of the antenna array sizes on the system performance. We consider the CAS architecture (i.e., M=1), and a DAS with M=4, and K=16. For the CAS, the average SNR is around 25dB, thus ensure most STAs are in high-SNR regime. The results are given in Fig. 3. (In all the figures, RT is short for ray-tracing, and IID for i.i.d. Rayleigh channel). The observations are summarized in the following.

The average IF capacity is stable due to the power assumption given in Section II. On the contrary, DPC, ZF and MBF all experience dramatic improvements when MN increases. The average capacity of the DAS is higher due to stronger received signal strength.

DPC, ZF, and MBF, provide data rates below IF case but tend to approach it as MN becomes larger. For example, for CAS in i.i.d. Rayleigh channel, DPC and ZF tightly approximate IF when $MN \geq 128$, i.e., around 8 times of K. The gaps are actually larger in ray-tracing channels. So, in order to achieve a similar data rate as in i.i.d. channels, many more antennas are needed.

The performance differences among the precoders also gradually vanish as MN increases. The interesting finding is that ZF

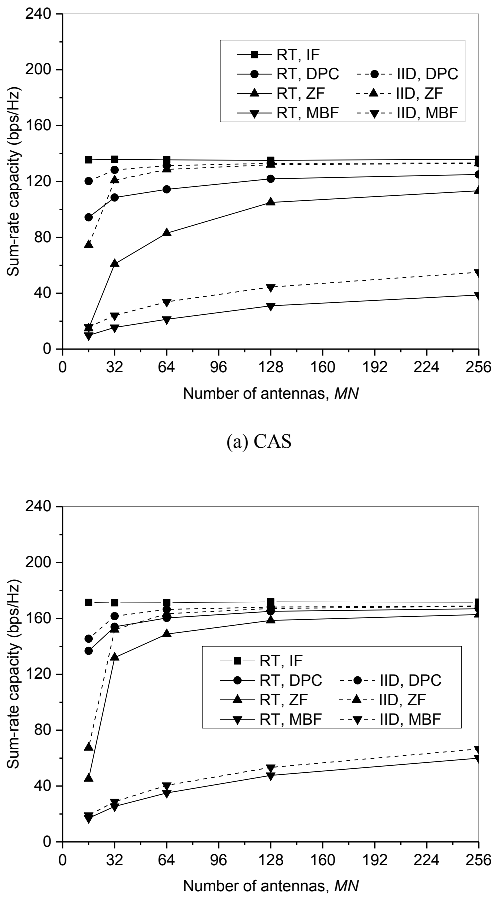

(a) CAS

(b) DAS ($M = 4$)

Fig. 3 Sum-rates versus total number of antennas with different configurations.

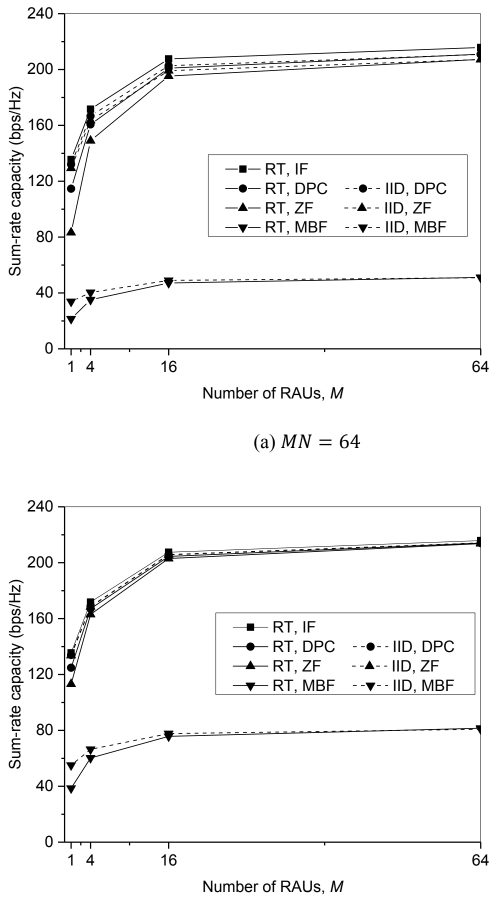

(a) $MN = 64$

(b) $MN = 256$

Fig. 4 Sum-rates versus the number of RAUs with the same total number of antennas.

can approximate the performance of DPC for a large MN, which confirms that simple linear precoders can provide close-to-optimum performance. MBF performs much poorer even when MN is very large, although theoretically it is also optimal under condition $MN \to \infty$. This suggests that precoders considering MUI mitigation should be more effective in practice, especially for the low frequencies, since the required antenna array size is much smaller.

Moreover, the outcome in ray-tracing channel is poorer than in i.i.d. Rayleigh channel. However, the gaps look smaller in DAS when we compare Fig. 3a and Fig. 3b. We further discuss this in the next subsection about the effect of antenna distributions.

B. Capacity Versus Antenna Distribution

Now we consider using the same number of antennas in total (i.e., MN is constant), to investigate the performance changes with different levels of antenna distribution. Specifically, different numbers of RAUs, M, are considered with optimized placement as we mentioned earlier. The other parameters are held the same. The number of STAs is K =16. Fig. 4 shows the results for MN=64 and 256, respectively.

It can be seen from the figures that a higher distribution level benefits the network from several perspectives. First, the overall sum-rates are increased. Second, the differences of linear precoders in comparison with DPC and IF are decreased. Third, the sum-rate gaps between ray-tracing channel and the ideal i.i.d. channel are smaller. The overall benefit is a compound effect of the macro- and the micro-diversity offered by DAS, which suggests great advantages of DAS over CAS.

Another point is that, the improvements saturate as M increases. From the results, we see that M=16 is already a satisfactory level. This is interesting for practice since it is not necessary to make all antennas distributed over the coverage area to get the best performance, while a small M can offer significant gains.

C. Capacity Versus Number of Co-scheduled STAs

Traditionally, the number of STAs K that can be supported simultaneously depends on the number of antennas at the AP. So, for large MIMO systems, the potential number of co-scheduled STAs is also large. However, as it is known that, to obtain low-level MUI, user scheduling and complex precoding are needed. The desirable strategy in large MIMO is to employ a much larger number of antennas than parallel spatial streams, in another word, let $MN \gg K$ [1]. As a result, low-complexity precoding can be used to get good performance. It is then interesting to know how large the ratio of MN/K should be. It has been reported in, e.g., [1], that the number of base station antennas should be at least 10 times the number of single-antenna STAs in CAS. The above analysis in this paper also supports this conclusion. However, for a DAS architecture, the statement does not hold. What we show later is that the total number of antennas needed in DAS is actually significantly less.

For the analysis in this subsection, we assume MN=256, and, M =1 (CAS) and M=16 (DAS). We vary K, to see how the sum-rate capacity changes. The other parameters are kept the same. The results are given in Fig. 5.

We can see that rather different results are obtained for CAS and DAS. Many more STAs can be supported in DAS than in CAS to approximately achieve the optimum IF capacity. The superiority is especially significant in the practical ray-tracing channels. For example, even when K=64, the STAs can still achieve close-to-optimum performance in DAS, which is not the case in CAS.

One major reason for the poor performance of CAS for large K is due to the compact antenna array which results in correlated channels when STAs are in line-of-sight condition and a poor-scattering channel is experienced. We can see that in i.i.d. Rayleigh channel, CAS still performs well but it is poor in ray-tracing channels. On the contrary, for DAS, the performance tends to be similar as in i.i.d. channels.

Some additional points are necessary to mention. We note that, the targeted K in a practical system may depend on other factors. For example, channel training overheads and the number of pilot sequences may limit K to a smaller number. For that reason, the CAS architecture may be sufficient to get the target performance as well. In addition, other considerations like the antenna array structure (e.g., cylinder array) and user scheduling, should be helpful for improving the performance. This is however out of the scope of this paper. So, the two architectures are equivalent for certain cases. The difference is that, to achieve the same performance, a CAS requires a sufficiently large antenna array, which turns into a large physical size which could lead to practical problems, e.g., form factor and installation issues. A DAS, on the other hand, needs fewer antennas, but requires a more sophisticated infrastructure to support antenna distributions, leading to higher installation cost. Indeed, the DAS architecture in particular with a higher distribution level, surpasses CAS significantly in terms of MU-MIMO capacity.

V. CONCLUSIONS AND FUTURE WORK

This paper analyzes the behavior of MU-MIMO with large antenna arrays in indoor WLAN, operating in the 2.4 GHz ISM band. We have considered the important factors related to the sum-rate performance, including precoding techniques, channel characteristics, and especially antenna configuration and deployment.

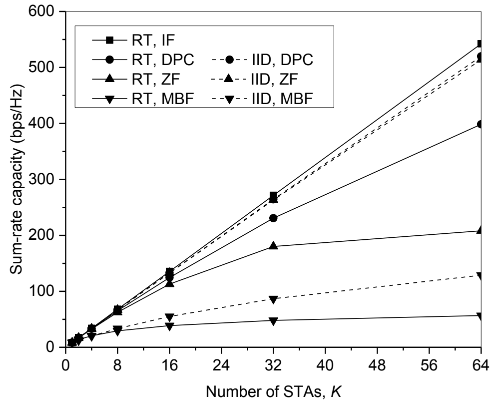

(a) CAS

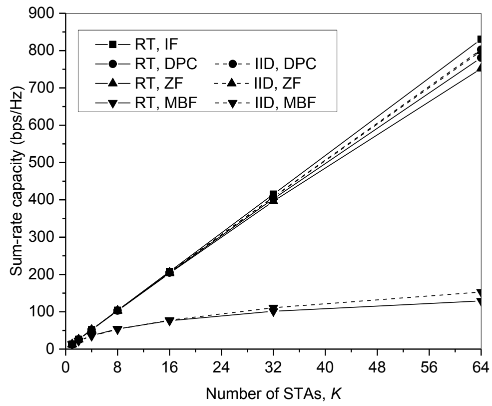

(b) DAS ($M = 16$)

Fig. 5 Sum-rates versus the number of co-scheduled STAs in CAS and DAS.

Although theoretically the upper bound capacity can be achieved by simple linear precoders as the number of antennas $MN \rightarrow \infty$, their performance differences are significant when MN is not infinite but assumes practical values, e.g., in the order of hundreds. Regarding precoding, ZF offers much better performance than MBF. This suggests MUI suppression is necessary in the precoding process, which should be considered for designing precoding techniques.

We also found that the DAS architecture significantly surpasses CAS in terms of capacity provisioning to a larger number of co-scheduled STAs. We can interpret that from several aspects. First, less antennas are needed with a DAS architecture, which is preferable in practice in terms of cost and complexity. Second, a higher antenna distribution level leads to better performance, but in fact a moderate level is satisfactory. For example, a balancing point in our analysis is $M = 16$, which results in an inter-RAU distance of around 16 m. Third, DAS is especially superior to CAS in practical channels due to the limited scattering and LOS conditions. This also means that in outdoor channels where the scattering is usually poorer than in indoor, DAS should provide a higher performance gain.

There are several important points we did not address and require further investigation. First, the effect of non-uniform user distributions, e.g., users are clustered at some locations. Second, one needs to consider multiple-AP cases, especially when inter-cell interference may exist due to the higher frequency reuse factor. This requires more sophisticated simulation of the wireless channels, and media access mechanisms. Third, one should take into account per antenna peak or average power constraints, or constant envelop transmission. Especially constant envelop transmission is currently a hot research topic for large MIMO systems [15]. Fourth, the backhaul-related issues for DAS may play a role, e.g., the optical fiber distortion needs to be considered.

REFERENCES

[1] F. Rusek, D. Persson, B. K. Lau, E. G. Larsson, T. L. Marzetta, O. Edfors, and F. Tufvesson, "Scaling up MIMO : Opportunities and challenges with very large arrays," *IEEE Signal Processing Magazine*, vol. 30, no. 1, pp. 40–60, Jan. 2013.

[2] E. G. Larsson, O. Edfors, F. Tufvesson, and T. L. Marzetta, "Massive MIMO for next generation wireless systems," *IEEE Communications Magazine*, vol. 52, no. 2, pp. 186–195, Apr. 2014.

[3] J. Hoydis, C. Hoek, T. Wild, and S. ten Brink, "Channel measurements for large antenna arrays," in *2012 International Symposium on Wireless Communication Systems (ISWCS)*, 2012, pp. 811–815.

[4] X. Gao, O. Edfors, F. Rusek, and F. Tufvesson, "Massive MIMO in real propagation environments," *arXiv preprint arXiv:1403.3376*, pp. 1–10, 2014.

[5] K. T. Truong and R. W. Heath, "The viability of distributed antennas for massive MIMO systems," in *Asilomar Conference on Signals, Systems and Computers*, 2013, pp. 1318–1323.

[6] J. Weng, X. Tu, Z. Lai, S. Salous, and J. Zhang, "Indoor massive MIMO channel modelling using ray-launching simulation," *International Journal of Antennas and Propagation*, vol. 2014, pp. 1–13, 2014.

[7] T. Koonen, "Fibre to the home/fibre to the premises: what, where, and when?," *Proceedings of the IEEE*, vol. 94, pp. 911–934, 2006.

[8] R. W. Heath, T. Wu, Y. H. Kwon, and A. C. K. Soong, "Multiuser MIMO in distributed antenna systems with out-of-cell interference," *IEEE Transactions on Signal Processing*, vol. 59, no. 10, pp. 4885–4899, 2011.

[9] K. Hosseini, W. Yu, and R. Adve, "Large-scale MIMO versus network MIMO for multicell interference mitigation," *IEEE Journal of Selected Topics in Signal Processing*, vol. 8, no. 5, pp. 930 – 941, 2014.

[10] A. Hekkala, M. Hiivala, M. Lasanen, J. Perttu, L. C. Vieira, N. J. Gomes, and A. Nkansah, "Predistortion of radio over fiber links: Algorithms, implementation, and measurements," *IEEE Transactions on Circuits and Systems*, vol. 59, no. 3, pp. 664–672, 2012.

[11] J. Lee and N. Jindal, "High SNR Analysis for MIMO Broadcast Channels: Dirty Paper Coding vs. Linear Precoding," *IEEE Transactions on Information Theory*, no. 2, p. 33, 2006.

[12] Q. Wang, Z. Cao, D. DebBarma, I. Niemegeers, S. Heemstra de Groot, and A. Lo, "Measurements and performance of large MIMO systems at 2.4 GHz for indoor WLAN," in *2014 IEEE 21st Symposium on Communications and Vehicular Technology in the Benelux (SCVT)*, 2014, pp. 35–40.

[13] J. Deissner, J. Hubner, D. Hunold, and J. Voigt, *RPS Radiowave Propagation Simulator*. Actix GmbH, 2008.

[14] E. Amaldi, A. Capone, M. Cesana, F. Malucelli, and F. Palazzo, "WLAN coverage planning: optimization models and algorithms," *2004 IEEE 59th Vehicular Technology Conference*, vol. 4, pp. 2219 – 2223, 2004.

[15] S. K. Mohammed and E. G. Larsson, "Per-antenna constant envelope precoding for large multi-user MIMO systems," *IEEE Transactions on Communications*, vol. 61, no. 3, pp. 1059–1071, 2013.

Qing Wang received his B.Eng. degree in Telecommunication Engineering from Xidian University, China, in 2009. In 2011, he obtained his M.E. degree in Information and Communication Engineering from National University of Defense Technology, China. He is currently working towards his Ph.D. degree in COBRA Research Institute at Eindhoven University of Technology, The Netherlands. His research interests include wireless and mobile communications, wireless indoor networks, WLAN and radio-over-fiber technologies.

Diptanil DebBarma was born in Agartala, India in 1986. He received his B.E from Sathyabama University, India in Electronics and Telecommunication in 2004 and graduated as one of the University Topper. He obtained his Masters (M.E) from the prestigious Indian Insti-tute of Science (IISc), India in Telecommunication, 2010, and was the recipient of the Ministry of Human Resource and Development (MHRD) scholarship. Currently he is pursuing his PhD at Eindhoven University of Technology (ECO group) working for the Dutch IOP-GenCom project MEANS. His research interest includes Wireless Communication, Wireless Network, Stochastic Network Control, Network Coding implementation in wireless MAC, Information Theory, MU-MIMO, Cooperative and Distributed MIMO.

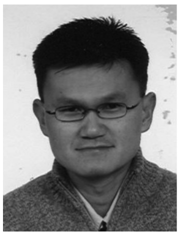

Anthony Lo received combined B.S. and B.E., and Ph.D. degrees in 1992 and 1996 from La Trobe University, Australia. He is currently a Principal Scientist at Huawei Technologies R & D Sweden. He was an assistant professor at Delft University of Technology and, prior to the academic appointment, he was a research engineer at Ericsson EuroLab working on UMTS/HSPA and LTE. His research interests include M2M Massive MIMO, communications, intelligent transportation systems, smart grids, and the wireless network cloud.

Ignas Niemegeers got an MSc degree in Electrical Engineering from the University of Gent, Belgium in 1970, an MSc in 1972 and a PhD degree in 1978 in Computer Engineering from Purdue University, USA. From 1978 to 1981 he was a system designer at Bell Telephone Mfg. Cy, Antwerp, Belgium. From 1981 to 2002 he was professor at the University of Twente, The Netherlands. From 1995 to 2002 he was Scientific Director of the Centre for Telematics and Information Technology (CTIT) of the University of Twente. From 2002 until 2012 he was chairman of the Telecommunications Department and professor in Wireless and 8 Mobile Communications at Delft University of Technology. Since August 2012 he is emeritus professor at Delft University of Technology and advisor to the Centre for Wireless Technology at Eindhoven University of Technology, The Netherlands. He was involved in many European research projects and reviewer for many projects. His present research interests are 5G, Radio-over-fiber networks, 60 GHz networking, energy-harvesting networks.

Sonia Heemstra de Groot holds M.Sc. degrees in Electrical Engineering from Universidad Nacional de Mar del Plata, Argentina and Philips International Insti-tute/ NUFFIC, The Netherlands. She obtained the Ph.D. degree in Electrical Engineering at the University of Twente, The Netherlands, in 1990. Since 2012 she is a full professor at Eindhoven University of Technology where she holds the part-time chair in Heterogeneous Network Architectures. Before she has had assistant and associate professor positions at the University of Twente and a full-professor position at the Delft University of Technology in Personal and Ambient Networking. After having worked some years as a senior researcher at Ericsson EuroLab, The Netherlands, she co-founded the Twente Institute for Wireless and Mobile where she has been Chief Scientist from 2003 to 2014. Her expertise and interests are in the areas of wireless and mobile communications, wireless networks, Internet of Things, wireless security, personal and ambient networks (co-inventor of the concept of personal networks and federations concept), vehicular networks, wireless indoor communications, and radio-based positioning techniques. She has coordinated and participated in many national and international research projects and has authored or co-authored more than 150 papers published in international journals or presented at international conferences.

Call for Papers

Special Issue on Applied Cryptography and Security

This special issue will focus on the area of applied cryptography and security, in particular on the following topics:

- **Applied Cryptography,**
- **Practical Cryptanalysis,**
- **Cryptographic Protocols,**
- **Security Mechanisms Deploying Cryptography.**

The Special Issue will accommodate journal versions of selected papers from SantaCrypt 2015, a Czech and Slovak workshop to be held in Prague, Czech Republic, on December 3-4, 2015. In addition, papers from open call are welcome.

Deadlines:

Submission of manuscripts: November 15, 2015.

Notification of authors about the evaluation: December 15, 2015.

Submission of camera ready versions of accepted papers: January 10, 2016.

Guest Editors:

VÁCLAV (VASHEK) MATYÁŠ is a Professor at the Masaryk University, Brno, CZ, and Vice-Dean for Foreign Affairs and External Relations, Faculty of Informatics. His research interests relate to applied cryptography and security, where he published over 150 peer-reviewed papers and articles, and co-authored several books. He was a Fulbright-Masaryk Visiting Scholar with Harvard University, Center for Research on Computation and Society in 2011-12, and previously he worked also with Microsoft Research Cambridge, University College Dublin, Ubilab at UBS AG, and was a Royal Society Postdoctoral Fellow with the Cambridge University Computer Lab. Vashek edited the Computer and Communications Security Reviews, and worked on the development of Common Criteria and with ISO/IEC JTC1 SC27. He received his PhD degree from Masaryk University, Brno and can be contacted at matyas AT fi.muni.cz.

ZDENĚK ŘÍHA is an Assistant Professor at the Masaryk University, Faculty of Informatics, in Brno, Czech Republic. He received his PhD degree from the Faculty of Informatics, Masaryk University. In 1999 he spent 6 months on an internship at Ubilab, the research lab of the bank UBS, focusing on security and usability aspects of biometric authentication systems. Between 2005 and 2008 he was seconded as a Detached National Expert to the European Commission's Joint Research Centre in Italy, where he worked on various projects related to privacy protection and electronic passports. He was involved in the ePassport interoperability group known as the Brussels Interoperability Group. Zdeněk has been working with the WG 5 (Identity management and privacy technologies) of ISO/IEC JTC 1/SC 27. Zdeněk's research interests include Android security, smartcard security, PKI, security of biometric systems and machine readable travel documents. Zdeněk can be contacted at zriha AT fi.muni.cz.

PAVOL ZAJAC is an Assistant Professor at the Slovak University of Technology in Bratislava, Faculty of Electrical Engineering and Information Technology, Slovakia (FEI STU). He received his PhD degree in Applied Mathematics from FEI STU. His main research focus is in the area of mathematical cryptology, including mathematical principles of cipher design, and algebraic cryptanalysis. He also works on various application projects, including efficient implementation of post-quantum cryptosystems, and improving privacy of user data on mobile devices. Pavol can be contacted at pavol.zajac AT stuba.sk.